Primary Photoprocesses Involved in the Sensory Protein for the Photophobic Response of *Blepharisma japonicum*

Johanna Brazard,[†] Christian Ley,[†] Fabien Lacombat,[†] Pascal Plaza,*[,†] Monique M. Martin,[†] Giovanni Checcucci,[‡] and Francesco Lenci[‡]

UMR 8640 CNRS-ENS-UPMC, Département de Chimie, Ecole Normale Supérieure, 24 rue Lhomond, 75005 Paris, France, and Istituto di Biofisica del CNR, Via G. Moruzzi 1, 56100 Pisa, Italy

Received: July 2, 2008; Revised Manuscript Received: September 8, 2008

We present new femtosecond transient-absorption and picosecond fluorescence experiments performed on OBIP, the oxyblepharismin-binding protein believed to trigger the photophobic response of the ciliate *Blepharisma japonicum*. The formerly identified heterogeneity of the sample is confirmed and rationalized in terms of two independent populations, called rOBIP and nrOBIP. The rOBIP population undergoes a fast photocycle restoring the initial ground state in less than 500 ps. Intermolecular electron transfer followed by electron recombination is identified as the excited-state decay route. The experimental results support the coexistence of the oxyblepharismin (OxyBP) radical cation signature with a stimulated-emission signal at all times of the evolution of the transient-absorption spectra. This observation is interpreted by an equilibrium being reached between the locally excited state and a charge-transfer state on the ground of a theory developed by Mataga and co-workers to explain the fluorescence quenching of aromatic hydrogen-bonded donor−acceptor pairs in nonpolar solvents. OxyBP is supposed to bind to an as yet unknown electron acceptor by a hydrogen-bond (HB) and the coordinate along which forward and backward electron transfer proceed is assumed to be the shift of the HB proton. The observed kinetic isotope effect supports this interpretation. Protein relaxation is finally proposed to accompany the whole process and give rise to the highly multiexponential observed dynamics. As previously reported, the fast photocycle of rOBIP can be interpreted as an efficient sunscreen mechanism that protects *Blepharisma japonicum* from continuous irradiation. The nrOBIP population, the transient-absorption of which strongly reminds that of free OxyBP in solution, might be proposed to actually trigger the photophobic response of the organism through excited-state deprotonation of the chromophore occurring in the nanosecond regime. Additional femtosecond transient-absorption spectra of OxyBP and peri-deprotonated OxyBP are also reported and used as a comparison basis to interpret the results on OBIP.

1. Introduction

Studying the primary photoprocesses involved in biological photoreceptors is a fascinating field that teaches us on the various solutions evolved by Nature in order to convert light into a biological signal. Most of the known light-sensing proteins belong to one of the following six families: rhodopsins, phytochromes, xanthopsins, cryptochromes, phototropins, and BLUF proteins.[1,2] The chromoprotein thought to be responsible for the step-up photophobic response of *Blepharisma japonicum*[3−7] nevertheless belongs to a different family. *B. japonicum* is a red-colored photophobic ciliated protozoan, the biology of which was described by Giese.[8] *B. japonicum* photoconverts into a blue, light-adapted, form upon continuous irradiation with weak intensities of white light (3−30 W m^{-2}).[5,9,10] Blue cells are particularly interesting because they still display the same phobic response as red cells[9] and because a stable chromophore−protein complex could be extracted from them.[6,7] This complex is made of a nonsoluble 200 kDa protein, noncovalently bound[11] to the chromophore identified as responsible for the photophobic response, namely oxyblepharismin (OxyBP, see chemical structure in Scheme 1).[4,5] OxyBP is a phenanthroperylene quinone derivative close to hypericin (Hyp, Scheme 1), a well-known photosensitizing agent.[12] OxyBP is also the photooxidized form of blepharismin (BP, Scheme 1), which is the photoreceptor molecule of the dark-adapted (red-colored) form of *B. japonicum*.[4,10] We will refer to the OxyBP-protein complex of *B. japonicum* as OBIP (OxyBlepharismin bInding Protein). The primary structure of OBIP is still unknown. In a preceding series of papers, we reported comparative subpicosecond transient-absorption studies of OBIP and OxyBP.[13−15] Electronically excited OxyBP in dimethyl sulfoxide (DMSO) was found to mainly decay in about 1 ns and to form the triplet state with a 25% yield. OBIP in a buffer solution exhibits a quite different and specific photoinduced behavior. First, the dynamics is much faster, displaying prominent 4 ps and 56 ps decay components over the entire experimental spectral range. A transient-absorption band centered around 680 nm was clearly observed for a pump−probe delay of 10 ps and was seen to vanish in the hundred-picosecond time scale. After this decay, the transient species dominating the longer times was seen to be very similar to free OxyBP in solution. These facts were interpreted in terms of the existence of two classes of chromoprotein complex. A so-called reactive one (rOBIP) was thought to give rise to the specific spectral features in the 640−740 nm region, and to the fast 4 and 56 ps dynamics. A second, nonreactive, complex (nrOBIP) would mostly behave like the free chromophore in solution. This long-lived species is believed to be free to rotate in all directions inside the protein pocket, even if the value of

* To whom correspondence should be addressed. Phone: +33 144322414. Email: Pascal.Plaza@ens.fr.
[†] UMR 8640 CNRS-ENS-UPMC.
[‡] Istituto di Biofisica del CNR.

10.1021/jp805815e CCC: $40.75
Published on Web 11/05/2008

SCHEME 1: Chemical Structures of Oxyblepharismin (OxyBP), Its Close Parent Hypericin (Hyp), and Its Natural Precursor Blepharismin (BP)[a]

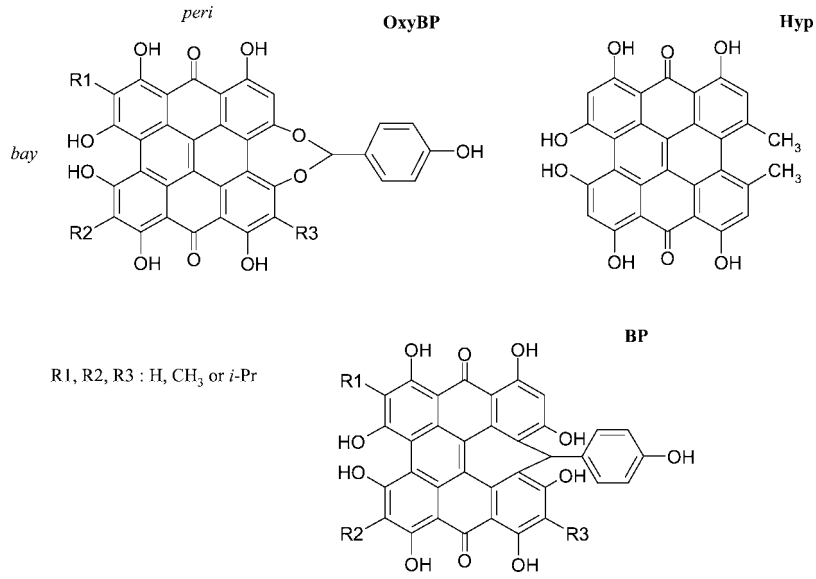

[a] The five isospectral forms of OxyBP and BP only differ by their alkyl lateral substituents (Ri).[41]

the rotational correlation time indicates that the local viscosity is about ten times higher than in ethanol.[13] We also showed that the distinctive 680 nm band bears a close similarity with the spectrum of the OxyBP radical cation.[14] This analogy points toward electron transfer as the primary photoinduced process in OBIP, in agreement with the previous proposal of Angelini et al.[16]

Several issues nevertheless remained unsolved. The details of the charge transfer reaction dynamics were in particular not completely resolved. A precursor state (called X_1) was tentatively identified at very short times but retained some of the spectral feature of its, putatively charge-transferred, successor (Y_1, produced with a 4 ps lifetime). It was not clear if X_1 was the primary excited-state of OBIP or some intermediate in the pathway toward Y_1. On the other hand, the choice of excitation wavelength (605 nm) was such that the main vibronic band of the stimulated-emission signal was partly obscured by scattering of the pump beam. This shed some doubts on the ground versus excited-state nature of species Y_1.

The present paper provides new experimental data aimed at answering these questions. Femtosecond transient absorption spectroscopy, with enhanced time resolution and sensitivity was performed on OBIP in order to access the subpicosecond time scale; deuterated OBIP (dOBIP) was also studied. The excitation wavelength was slightly blue-shifted (560 nm for OBIP and 555 nm for dOBIP) in order to avoid pump-light scattering in the stimulated-emission region. Time-resolved fluorescence measurements were also carried out with a streak camera in order to identify emitting species along the overall kinetics. The observations will here be interpreted with the help of an improved model, and a tentative quantitative description will be proposed to support it. New elements concerning the issue of the relation between the excited-state behavior of OBIP and the photophobic response of *B. japonicum* will be given. In addition, several complementary measurements have been performed to calculate the fluorescence quantum yields of OBIP, dOBIP, and free OxyBP in aqueous solution (protonated and deprotonated, ordinary and deuterated). A comparison of the excited-state behaviors of protonated and deprotonated free OxyBP in aqueous solution is also given.

2. Materials and Methods

2.1. Samples Preparation. Red *Blepharisma japonicum* cells were grown in the dark at 23 °C in the presence of *Enterobacter aerogenes* as food supply. Blue (light adapted) cells were produced by in vivo photoconversion under a low intensity cold white lamp (below 10 W m^{-2}) for a few days. Blue cells were washed, collected by low speed centrifugation, and resuspended in a 20 mmol L^{-1} sodium cholate (NaCh) solution. The OBIP chromoprotein was purified by liquid chromatography of this preparation on a hydroxyapatite column.[7,13,17] The protocol closely follows the one described by Checcucci et al.,[17] which proved to yield samples mainly containing the 200 kDa (SDS-PAGE determination) OBIP protein. The purity of our sample was not quantified. It was then concentrated by means of Pall (East Hills, USA) centrifugable membrane filters (30 kDa cutoff) in order to achieve an absorbance of ~0.85 at the absorption maximum (605 nm), over an optical path of 1 mm. The pH of the 0.2 mol L^{-1} phosphate buffer, containing 10 mmol L^{-1} NaCh, was adjusted at 7.4 (this buffer will be referred to as PBC, phosphate buffer with cholate).

Deuterated OBIP (dOBIP) was obtained by diluting a concentrated OBIP solution in deuterated phosphate buffer and reconcentrating it over centrifugable membrane filters. The procedure was repeated until the remaining ordinary water content was less than 1% vol/vol.[18] In deuterated solution, the experimentally linear correlation between pD and pH reads as $pD = pH + 0.4$.[19,20] In order to obtain similar acido-basic conditions as the ordinary buffer, pD of the deuterated phosphate buffer was adjusted at 7.8 (the pH meter was corrected for the isotope effect[21]). The absorbance of the final deuterated OBIP sample was ~0.7 at the absorption maximum (600 nm). Heavy water, 99.9 atom % D, was purchased from Aldrich (deuterated PBC will be noted dPBC).

Free chromophore (blepharismin) was extracted in acetone from dark-adapted (red) cells, dried, and photooxidized in vitro to OxyBP by irradiation for a few hours with a dim light (below 10 W m^{-2}). The sample was finally purified by HPLC as previously described.[22] To overcome the poor solubility of OxyBP in water, leading to the formation of polydispersed

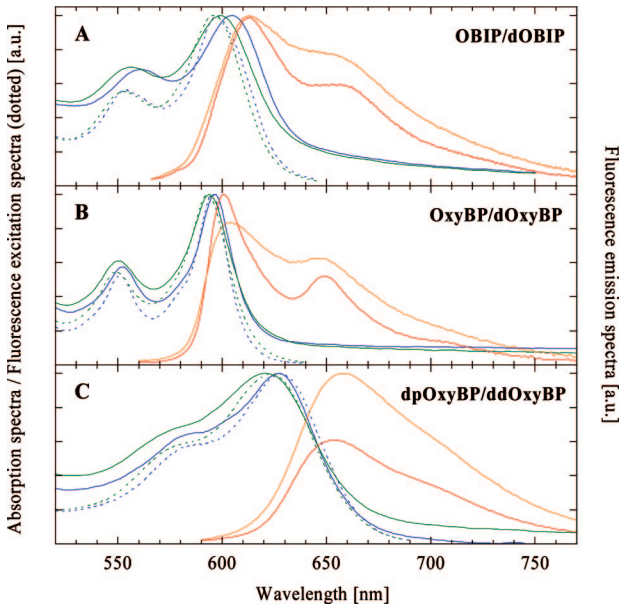

Figure 1. Steady-state absorption, fluorescence excitation, and fluorescence emission spectra of the following species in aqueous solutions: (A) OBIP and deuterated OBIP (dOBIP), (B) OxyBP and deuterated OxyBP (dOxyBP), (C) peri-deprotonated OxyBP (dpOxyBP) and peri-dedeuterated OxyBP (ddOxyBP). The absorption spectra of the ordinary species are plotted in blue and those of the deuterated species in green. The fluorescence excitation spectra are plotted in dotted lines, with the same color code. The fluorescence emission spectra are plotted in red for ordinary species and in orange for deuterated species. The detection (respectively excitation) wavelengths used for recording the fluorescence excitation (respectively emission) spectra are found in Table 1. All spectra have been normalized at their maxima, except for the weakest (at maximum) fluorescence emission spectrum of each view: the ratio of the two integrated fluorescence emission spectra is equal to the ratio of the fluorescence quantum yields of the corresponding species.

aggregates,[23] spectroscopic-grade ethanol (Merck) was added to the phosphate buffer at pH 7.4, containing 75 mmol L^{-1} NaCh. The final ethanol content was 1% vol/vol (this solution will be referred to as PBCE, phosphate buffer with cholate and ethanol). The use of both NaCh and ethanol in these proportions reduces the amount of aggregates to a relatively low level, as shown by the correctly structured absorption spectrum (Figure 1B, to be compared to the absorption spectra of OxyBP in pure ethanol and in phosphate buffer saline without ethanol[23]), although some nonfluorescent scattering background remains. The deuterated form of oxyblepharismin is noted dOxyBP. It was obtained by dissolving the free chromophore in a deuterated phosphate buffer at pD 7.8 containing 75 mmol L^{-1} NaCh (this deuterated solution will be noted dPBC).

On the other hand, solutions of peri-deprotonated OxyBP (dpOxyBP) were prepared by setting the pH at 14.3 with a 2.1 mol L^{-1} NaOH solution, containing 50 mmol L^{-1} NaCh and 1% vol/vol EtOH (this aqueous solution will be referred to as WCE, water with cholate and ethanol). These conditions are in good agreement with previous studies on hypericin, a parent molecule (Hyp, see Scheme 1), situating the pK_a of the perihydroxyls of this very similar compound around 11.[12,24,25] Since the pK_a of the bay hydroxyl of Hyp was reported around 2,[25] pH 14.3 ensures that most of the oxyblepharismin molecules should be bay monodeprotonated and peri-dideprotonated. It may be noted that the hydroxyl function of the lateral phenol of OxyBP, linked to the phenanthroperylene ring by two ether oxide groups, is also expected to be deprotonated at such pH (typical pK_a of a para-substituted phenol: 8−10[26]). This effect is nevertheless not expected to influence the spectroscopy of the molecule because the main aromatic ring is not conjugated to the lateral phenol. In the same way, peri-dedeuterated OxyBP (ddOxyBP) solutions were prepared in heavy water at pD ≈ 14.7, containing 75 mmol L^{-1} NaCh (this deuterated solvent will be noted dWC).

2.2. Steady-State Spectroscopy. Optical absorption spectra were measured using a Safas UV-mc2 dual-beam spectrophotometer. Corrected fluorescence emission and excitation spectra were measured with a Jobin-Yvon Fluoromax-3 spectrofluorometer.

Fluorescence quantum yields were calculated[27] in aerated conditions both with rhodamine 101 (fluorescence quantum yield: $\Phi_{fluo} = 1$ in both deaerated and aerated solutions[28,29]) and cresyl violet ($\Phi_{fluo} = 0.54$ in the presence of dioxygen[30]) as reference compounds. The values given in this work are the average of the two measurements. An estimate of the scattering background present on the absorption spectra was subtracted prior to correcting the sample absorbance at the excitation wavelength. The fluorescence excitation wavelengths were 560 nm for OBIP and dOBIP, 553 nm for OxyBP and dOxyBP, and 585 nm for dpOxyBP and ddOxyBP.

For the fluorescence excitation spectra, the emission wavelengths were fixed at 650 nm for OBIP, dOBIP, and OxyBP, 647 nm for dOxyBP, 700 nm for dpOxyBP. and 695 nm for ddOxyBP.

2.3. Transient Absorption Spectroscopy. Femtosecond transient absorption spectra were recorded by the pump-continuum-probe technique. The source was an amplified Ti:Sapphire laser system (Tsunami and Spitfire, Spectra Physics), delivering 50 fs pulses at 810 nm and 1 kHz. Part of this beam was used to run a 405 nm pumped noncollinear two-stage optical parametric amplifier (NOPA, Clark-MXR) in order to generate ∼35 fs pump pulses (after compression), tuned at the secondary absorption maximum of the pigment (560 nm for OBIP, 555 nm for dOBIP, 552 nm for OxyBP in PBCE, and 590 nm for deprotonated OxyBP in WCE). An energy of 0.27 μJ (per pulse) of this beam was focused by a 90° off-axis parabolic mirror onto a 0.048 mm^2 section of the OBIP sample. Energies of 0.26, 0.33, and 0.18 μJ were focused onto a 0.35 mm^2 section for the dOBIP, OxyBP, and dpOxyBP experiments, respectively. Care was taken to check that this fluence lies in the linear regime and does not induce multiphotonic excitation such as those previously reported for Hyp[11] or *O*-hexamethoxyhypericin.[31] The polychromatic probe beam (single-filament continuum extending from near-UV to near-IR nm) was generated by focusing a few μJ $pulse^{-1}$ of the 810 nm beam on a moving CaF_2 plate. The transmitted 810 nm wavelength was rejected from the probe by a 1 mm Schott BG40 bandpass filter. The continuum was split into a sample and a reference beam. The sample probe beam was focused by a 90° off-axis parabolic mirror onto the sample cell and crossed the pump beam at an angle of ∼5°. The linear polarizations of the pump and probe beams were set at the magic angle. The sample solutions were contained in 1 mm thick fused-silica cuvettes. Photolysis was avoided by continuously moving the sample cell up and down; the steady-state absorbance of the samples was checked to remain constant during the experiments. The probe beam was delayed with respect to the pump beam by an optical delay line. Reference and sample probe beams were finally directly focused onto the entrance slit of an imaging spectrograph (Acton SP300i, 150 grooves/mm^{-1}, spectral resolution better than 2 nm). The spectra were recorded at 333 Hz on a CCD matrix detector (Spec-10 100B, Roper Scientific, 100 × 1340 pixels) and accumulated

TABLE 1: Spectral Positions of the Steady-State Absorption, Fluorescence Excitation, and Fluorescence Emission Maxima of OBIP, Deuterated OBIP (dOBIP), OxyBP, and Deuterated OxyBP (dOxyBP), Peri-Deprotonated OxyBP (dpOxyBP), and Peri-Dedeuterated OxyBP (ddOxyBP) in Aqueous Solutions (see Details in *Material and Methods*)[a]

	OBIP	dOBIP	OxyBP	dOxyBP	dpOxyBP	ddOxyBP
absorption maximum (nm)	605.0	599.0	596.5	594.0	627.5	621.0
fluorescence excitation maximum (nm)	597.5	595.5	595.0	593.0	628.0	623.0
detection wavelength (nm)	*650*	*650*	*650*	*647*	*700*	*695*
fluorescence emission maximum (nm)	613.0	613.0	601.0	604.0	654.0	658.0
excitation wavelength (nm)	*560*	*560*	*553*	*553*	*585*	*585*
fluorescence quantum yield	0.023 ± 0.004	0.029 ± 0.005	0.098 ± 0.009	0.15 ± 0.01	0.15 ± 0.06	0.28 ± 0.08

[a] The detection (resp. excitation) wavelengths used for recording the fluorescence excitation (resp. emission) spectra is indicated in italics under the fluorescence excitation (resp. emission) maximum. The fluorescence quantum yields of each species are given in the last line, with corresponding errors.

over 3000 pump shots. Two accumulated spectra were averaged for each pump−probe delay. The differential absorbance spectra (ΔA) were corrected from the chirp of the probe beam, arising from group velocity dispersion in the material media it passes through before reaching the sample. Since scattering of the pump beam obscures the signal in the spectral region corresponding to excitation, the corresponding part of the differential spectra was removed prior to data analysis and masked in the figures.

The complete set of experimental data was globally fitted to a sum of exponential functions by the following method. Singular value decomposition (SVD)[32] was performed on the matrix containing the two-way chirp-corrected data (wavelength and time). In a first step, the kinetic vectors associated to the seven largest singular values (weighted by their corresponding singular values) were then simultaneously fitted to a sum of exponentials, convoluted by a Gaussian function representing the response function of the apparatus. The fwhm of the latter was found to be of the order of 100 fs. The presence of a cross-phase modulation (XPM) artifact during pump−probe overlap was empirically taken into account by adding the sum of the same Gaussian function and its time derivative. As this description of the XPM artifact is only approximate, we noted that the amplitude of any exponential component lying in the sub-500 fs regime could be slightly contaminated by remains of the incompletely fitted artifact. The difficulty was solved by running a second SVD analysis on a truncated data matrix, where times below 200 fs were removed. The kinetic vectors associated to the five largest singular values were then fitted by using parameters (width of the Gaussian function, time location of the pump−probe maximal overlap) obtained in the preceding step. The decay-associated difference spectrum (DADS) of each time component was finally calculated over the entire experimental spectral range.[33] The amplitude of the residue (2D-rms) was of the order of ± 0.3 mOD.

Note that such a multiexponential global approach is one convenient way to describe and quantify the transient behavior of the system. It also indirectly implies that the signal at all wavelengths may be explained by some (as yet undetermined) kinetic scheme, involving a limited number of transient species (compartments) linked by first order reaction rates. The knowledge of those rates as well as the intrinsic spectra associated to each compartment would lead to the lifetimes of the multiexponential fit. This procedure may face technical difficulties when the transient absorption spectra are found to display substantial time-dependent shift of the bands, such as those observed in solvation dynamics or cooling phenomena. In those cases, a discrete compartmental model is not adapted. However if the shifts are small as in some of the cases treated in this work (free pigments; the chromoprotein does not exhibit shifts), the procedure can converge and exhibit DADS which must be interpreted in terms of the underlying continuous shift phenomenon.

2.4. Time-Resolved Fluorescence Measurements. For picosecond time-resolved fluorescence experiments, the excitation source was a homemade subpicosecond dye laser system described elsewhere.[34] The OBIP sample, held in a 1 mm cuvette, was excited with 4.5 μJ of the 600 fs pulses at 566 nm and at a repetition rate of 2.5 Hz. The back-emitted fluorescence was collected at $\sim$165° from excitation, through a polarizer set at the magic angle. It was then analyzed with a streak camera (RGM-SC1, ARP-Optronis), the maximal time resolution of which is 4 ps. A 24 "wratten" Kodak filter was used to remove scattering of the excitation beam. All wavelengths greater than 580 nm were thereby integrated. A properly advanced reference pulse at 566 nm and the fluorescence decay were simultaneously recorded on the same camera image (at different positions along the entrance slit direction). An accumulated image was obtained by automatically superimposing the reference pulse of 1000−4000 single-shot images, in order to eliminate the jitter in triggering the camera sweep. The fluorescence decays were fitted to a sum of exponential functions, convoluted with a response function. The response function was assumed to be the sum of two Gaussians, the widths, time shift, and relative amplitudes of which being adjustable parameters. The main and short one is the genuine linear response function, which includes the fact that the photons emitted from different depths of the sample cuvette reach the camera at different times. With the fastest sweeping speed, the fwhm of this response was found to be 10 ps. The minor and long Gaussian empirically takes into account a background signal only observed with long-lived fluorescence. It may be an artifact due to the presence of remaining photoelectrons in the camera tube after the end of the sweep.

3. Results

The results are organized as follows: steady-state spectroscopy of all the compounds is first presented (Section 3.1), then transient absorption spectroscopy of the free pigments (Section 3.2) and of the chromoprotein (Section 3.3) are reported. The time-resolved fluorescence data on OBIP are shown last (Section 3.4).

3.1. Steady-State Spectroscopy. In this section we report steady-state absorption and fluorescence measurements complementing the already available data on OBIP and OxyBP.[13,14,16,17,35] We present new measurements on ordinary and deuterated OBIP (dOBIP), ordinary and deuterated oxyblepharismin (OxyBP and dOxyBP, respectively), as well as peri-deprotonated and peri-dedeuterated OxyBP (dpOxyBP and ddOxyBP, respectively), in aqueous solutions (PBCE, dPBC, WCE, and dWC). Figure 1 displays the corresponding steady-state absorption, fluorescence excitation, and fluorescence emission spectra. The scat-

tering background observed in the red part of the absorption spectra is assigned to aggregated proteins in the case of OBIP and dOBIP, and to incompletely solubilized chromophore in the case of the OxyBP, dOxyBP, dpOxyBP, and ddOxyBP. Table 1 gives the spectral position of the maximum of each of those spectra, together with the detection (respectively excitation) wavelengths used for recording the fluorescence excitation (respectively emission) spectra.

The absorption spectra of the chromoprotein (OBIP, dOBIP) and the associated chromophore (OxyBP, dOxyBP) display a common vibrational progression with a principal and a secondary maximum, respectively situated around 600 and 560 nm (see Table 1 for exact values). The corresponding vibrational frequency lies in the range of 1300 cm^{-1}. The fluorescence emission spectra are mostly mirror images of the absorption spectra, with first and secondary maxima located around 610 and 650 nm respectively and an associated vibrational frequency in the range of 1100 cm^{-1}. The mirror image symmetry is best respected in the case of OxyBP in PBCE, as is known to be the case for OxyBP and Hyp in organic solvents.[14,36] In the case of dOxyBP in dPBC, the vibrational progression of the fluorescence spectrum is much less clear than that of the absorption spectrum: the main peak is significantly broadened on its red side and the minimum between the two maxima (634 nm) is shallower. For OBIP in PBC, a similar although less pronounced trend can be seen with a shallower minimum at 642 nm as compared to the absorption spectrum. The effect is clearer as one compares the fluorescence emission spectrum of OBIP to its fluorescence excitation spectrum. The fluorescence/absorption dissymmetry is manifest in the case of dOBIP in dPBC, the main fluorescence peak being broadened on its red side and the secondary maximum being reduced to a shoulder.

The absorption spectrum of dpOxyBP is red-shifted by 31 nm as compared to that of OxyBP while the shift of the fluorescence spectrum is 53 nm. Similar values are observed for ddOxyBP as compared to dOxyBP.

It is worth noting that deuteration induces a slight blue shift (by a few nanometers) of the absorption and fluorescence excitation spectra, while the fluorescence emission spectrum either does not shift or slightly shifts toward the red. As noted above, deuteration also noticeably broadens the structure of the fluorescence emission spectrum of OxyBP and OBIP.

Both the absorption and fluorescence spectra of OBIP are red-shifted by 8.5 and 12.0 nm, respectively, as compared to those of OxyBP and significantly broadened. It is interesting to note that the fluorescence excitation spectrum of OBIP is significantly narrowed and blue-shifted as compared to the corresponding absorption spectrum. One may appreciate from Figure 1 that the removal of the scattering background in the fluorescence excitation spectrum may slightly contribute to the observed blue shift but cannot account for all of it. This observation indicates that the red edge of the absorption spectrum of OBIP yields a weaker fluorescence than the blue edge.

Fluorescence quantum yields (average value calculated with rhodamine 101 and cresyl violet as reference compounds) are given in the last line of Table 1. The fluorescence quantum yield of OBIP (2.3%) is smaller than that of OxyBP (9.8%) by a factor of 4, in qualitative agreement with previous determinations[14,17] and the existence of specific fast deactivation processes in OBIP.[13,14] The fluorescence quantum yield of the corresponding deuterated species are found to be somewhat larger (2.9% for dOBIP and 15% for dOxyBP), the dOBIP to dOxyBP fluorescence yield ratio being of the order of five. Significantly larger

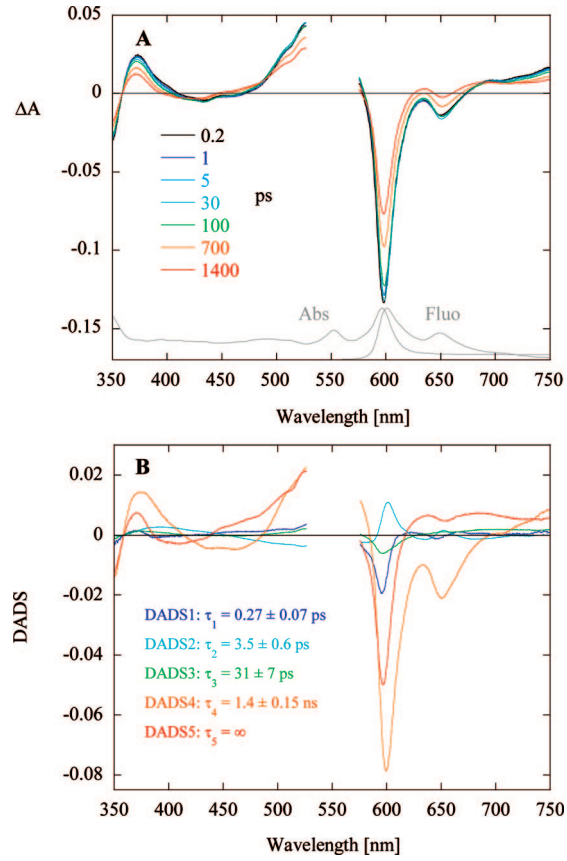

Figure 2. (A) Overview of the transient absorption spectra of solution of OxyBP in PBCE, excited at 552 nm, at a few selected pump−probe delays between 0.2 ps and 1.4 ns. The steady-state absorption and fluorescence spectra are reminded in gray line at the bottom of the graph. (B) Decay-associated difference spectra (DADS) attached to each of the five time components found in the global analysis of the transient absorption spectra.

fluorescence quantum yields were measured for the deprotonated/dedeuterated free chromophore (15.1% for dpOxyBP and 27.6% for ddOxyBP).

3.2. Transient Absorption Spectroscopy of OxyBP and dpOxyBP. Figure 2A displays an overview of the transient absorption spectra of an aqueous solution of OxyBP (containing 75 mmol L^{-1} NaCh and 1% vol/vol ethanol to solubilize the molecule at pH 7.4), excited at 552 nm, at a few selected pump−probe delays between 0.2 ps and 1.4 ns. As previously reported with a lower time resolution for OxyBP and Hyp in DMSO[13] (and similarly for Hyp in DMSO[11]), one observes relatively little spectral evolution in the subns regime. The sharp negative peak centered at 598 nm corresponds to the overlap of the main bleaching and the main stimulated-emission bands. The secondary bleaching minimum (~550 nm) is hidden in the region that was masked because of the pump beam scattering while the secondary stimulated-emission minimum is clearly apparent at 650 nm. The start of an additional bleaching band is detected below 360 nm. Two positive maxima are identified around 372 and 525 nm, which arise from the overlap of the above-mentioned negative bands and a broad transient absorption continuum, extending over most of the experimental spectral range.

Upon careful examination one sees a very slight red shift (~0.5 nm) of the two negative bands in the first few picoseconds. In the subnanosecond regime the decay of the excited-state spectrum appears mostly homothetic, although at 1.4 ns a growth of a positive signal is readily visible at 634 nm. A couple

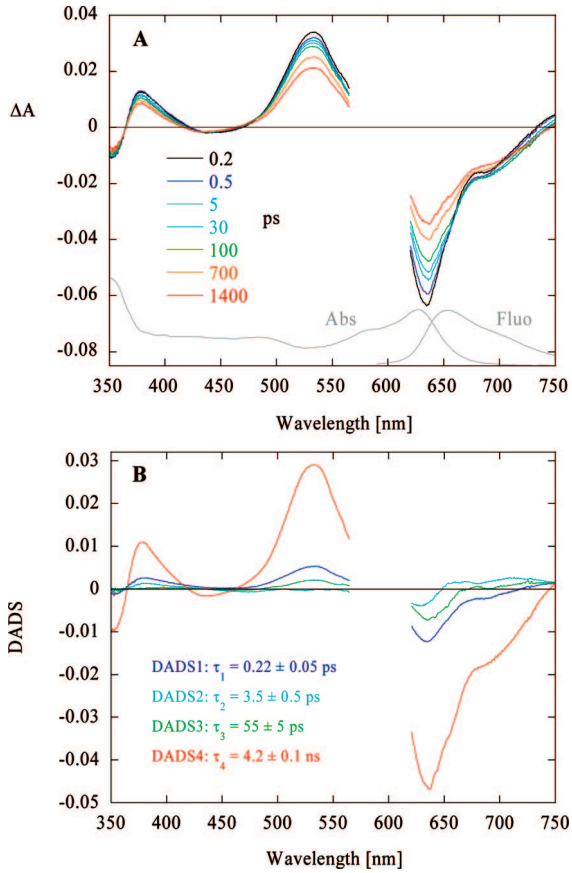

Figure 3. (A) Overview of the transient absorption spectra of solution of peri-deprotonated OxyBP in WCE, excited at 590 nm, at a few selected pump−probe delays between 0.2 ps and 1.4 ns. The steady-state absorption and fluorescence spectra are reminded in gray line at the bottom of the graph. (B) Decay-associated difference spectra (DADS) attached to each of the four time components found in the global analysis of the transient absorption spectra.

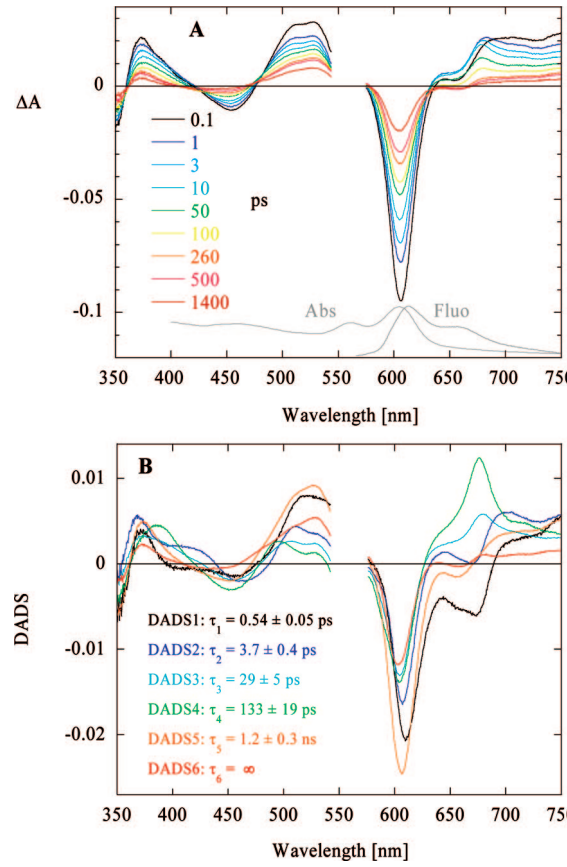

Figure 4. (A) Overview of the transient absorption spectra of solution of OBIP in PBC at pH 7.4, excited at 560 nm, at a few selected pump−probe delays between 0.1 ps and 1.4 ns. The steady-state absorption and fluorescence spectra are reminded in gray line at the bottom of the graph. (B) Decay-associated difference spectra (DADS) of the six time components found in the global analysis of the transient absorption spectra.

of isosbestic points (414, 489, and more unclearly around 703 nm) are observed at long times. Since their differential absorbance values are different from zero (trivial case arising from the decay of a single excited-state to the ground state), they most likely reveal the formation of a long-lived species.

The global analysis of the data reveals four exponential components followed by a plateau. The lifetimes of the exponentials are the following: 0.27 ± 0.07 ps, 3.5 ± 0.6 ps, 31 ± 7 ps, 1.40 ± 0.15 ns (standard errors as provided by the software (Origin 7.0) used for nonlinear fitting of the SVD kinetic vectors). Figure 2B shows the decay-associated difference spectra (DADS), that is, the preexponential factor spectra associated to each time component.

The transient absorption spectra of peri-deprotonated OxyBP in WCE (at pH≈14.3) after excitation at 590 nm are represented in Figure 3A. The overall spectral structure reminds that of OxyBP in WCE with a large red shift and broadening of the bleaching and stimulated-emission bands, as expected from the steady-state spectra. The main bleaching and stimulated-emission merged band appears at 635 nm and a stimulated-emission vibronic structure is visible as a shoulder around 690 nm. The transient-absorption bands seen at 378 and 532 nm are quite similar to the corresponding one of OxyBP. The global decay of the spectra is slower than for OxyBP and does not involve much changes of shape in the ns/subns regime. During the first 100 ps, some changes are nevertheless visible above 650 nm. The signal decreases on the blue side of the steady-state fluorescence spectrum while it rises of the red side. The signal remains nearly constant around 662 nm.

As far as kinetic analysis of the data is concerned, the best fit would involve four exponential components followed by a plateau. However, the slowest component of such a fit is so slow (3.4 ns), as compared to our observation window, that its DADS and that of the plateau are ill-defined. We therefore reduced the fitting function to a sum of four exponentials. The lifetimes are the following: 0.22 ± 0.05 ps, 3.5 ± 0.5 ps, 55 ± 5 ps, 4.2 ± 0.1 ns. Figure 3B displays the corresponding DADS. It must however be kept in mind that the 4.2 ns component could in fact be the average of a somewhat shorter decay (3−4 ns) followed by a plateau.

3.3. Transient Absorption Spectroscopy of OBIP and dOBIP. Figure 4A plots a selection of transient-absorption spectra of OBIP, after excitation at 560 nm, for pump−probe delays lying between 0.1 and 1400 ps. It is most interesting that the present experimental setup allows the detection of new spectro-dynamic features, as compared to previously published results,[13,14] at very short times (<1 ps) and provides a substantially enhanced S/N ratio over the entire spectral and temporal range. We confirm here that the transient spectra of OBIP display unique both temporal and spectral characteristics. Although their overall shape reminds that of free OxyBP with a large bleaching and stimulated-emission merged peak at 606 nm and transient-absorption bands at 373 and 528 nm, a specific behavior is in particular observed in the 630−750-nm range. At 0.1 ps, a nearly flat transient-absorption band extends from

688 to 750 nm, and the sharp short-wavelength edge of it is most likely arising from the secondary peak of the stimulated-emission signal. This band rapidly evolves in about 1 ps and produces a local maximum at 683 nm which further develops into a well-defined peak at 678 nm in some 10 ps. This fast evolution is accompanied by a decay of the whole spectrum below 635 nm. This decay is however not homothetic, as for example revealed by the presence of a nontrivial ($\Delta A \neq 0$) temporary isosbestic point at 482.5 nm, or by the blue shift (~3 nm) of the local bleaching minimum at 455 nm. Subsequently, in about 500 ps the 678 nm peak completely disappears while a net gain band appears at 655 nm. At the same time, the major bands further decay. The evolution is again nonhomothetic; the bleaching feature at 453 nm tends to vanish and the transient-absorption band that initially displays two comparable peaks at 510 and 528 nm tends to favor the 528 nm one with respect to the other.

Global analysis of the data is best performed with five exponential components and a plateau. The lifetimes of the exponentials are the following: 0.54 ± 0.05 ps, 3.7 ± 0.4 ps, 29 ± 5 ps, 133 ± 19 ps, 1.2 ± 0.3 ns. Figure 4B gives the corresponding DADS. As one normalizes DADS1 to DADS5 at the maximum of the main negative peak (not shown), one observes that this band most probably contains a stimulated-emission contribution on its long wavelength side in all five cases. This suggests that an emitting species decays with each of these time components, which could not be ascertained in previous works on this subject. This conclusion is further confirmed in Section 3.4 where the results of time-resolved fluorimetry will be presented. It can also be noted that bleaching is also contributing on the short wavelength side of the main negative band of each of the five time components, indicating that ground-state recovery involves all those exponentials.

The transient-absorption spectra of a deuterated OBIP sample (dOBIP), that is, OBIP in deuterated PBC, were also recorded with femtosecond excitation at 555 nm (Figure 5A). These spectra essentially show the same type of spectro-temporal behavior as the ones of OBIP, in particular with the ultrafast growth of a positive band around 676 nm which subsequently decays in the subnanosecond regime. The overall evolution rates are nevertheless substantially reduced, as confirmed by global analysis. The complete set of data is here best described by the sum of six exponentials followed by a plateau. The corresponding lifetimes are the following: 0.18 ± 0.04 ps, 1.1 ± 0.1 ps, 6.8 ± 0.6 ps, 47 ± 13 ps, 184 ± 33 ps, 3.5 ± 6 ns. The last component and subsequent plateau are obviously not well determined because of the limited observation window our experiment (1.4 ns). However we did not simplify the fitting function to six exponentials without a plateau because the present fit allows an approximate one-to-one correlation of the DADS of dOBIP (Figure 5B; the DADS of the plateau was omitted) to those of OBIP (Figure 4B). It thus appears that the 0.18 and 1.1 ps components of dOBIP should be compared to the 0.54 ps component of OBIP. Similarly the 6.8 ps, 47 ps, 184 ps, and 3.5 ns components of dOBIP should correspond to the 3.7 ps, 29 ps, 133 ps, and 1.2 ns components of OBIP, respectively (see Table 2).

3.4. Time-resolved Fluorescence Spectroscopy of OBIP. Figure 6 displays spectrally integrated fluorescence decays of a solution of OBIP in PBC, after 600 fs excitation at 566 nm, detected by a streak camera. The three kinetic traces correspond to three sweeping rates with increasing observation time window and decreasing time resolution. The decays were globally fitted to the sum of five shared exponentials, each trace involving convolution by its own response function. The best fit includes a short component that could not be resolved (<10 ps) and the following four subsequent lifetimes: 21 ± 1 ps, 112 ± 1 ps, 891 ± 16 ps, 4.4 ± 0.1 ns. The relative weights of the four resolved components are: 15.5%, 15.8%, 29.1% and 39.6%, respectively.

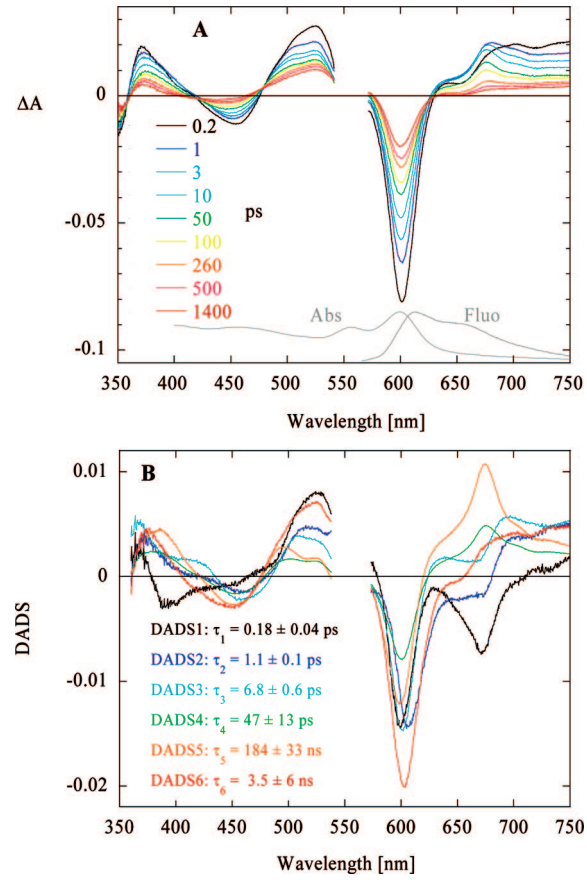

Figure 5. (A) Overview of the transient absorption spectra of solution of dOBIP in dPBC at pD 7.8, excited at 555 nm, at a few selected pump−probe delays between 0.2 ps and 1.4 ns. The steady-state absorption and fluorescence spectra are reminded in gray line at the bottom of the graph. (B) Decay-associated difference spectra (DADS) of the six exponential components found in the global analysis of the transient absorption spectra (the ill-defined plateau was omitted).

The unresolved short component could well correspond to the 3.7 ps detected by transient-absorption spectroscopy (Trabs). The 21.3 and 112 ps fluorescence components are reasonable matches for the 29 and 133 ps Trabs components, respectively. The 891-ps and 4.4-ns fluorescence components are likely to be related to the 1.2-ns component and plateau found by Trabs, although a one-to-one correspondence may not be ascertained. Rather large errors are indeed attached to nanosecond Trabs components because of the limited observation window (three long time components might for example appear as two intermediate ones). Table 2 summarizes the correspondence between Trabs and time-resolved fluorescence data. The fluorescence experiments thus confirm that the second to fifth Trabs components involve emitting species (see section 3.3).

4. Discussion

In this discussion, the excited-state behaviors of the free pigments, protonated and peri-deprotonated, are first compared (Section 4.1) before examining issues related to the OBIP chromoprotein. The following questions are then treated:

TABLE 2: Comparison of the Exponential Time Components Obtained by Analysis of the Transient-Absorption (Trabs) Spectra of OBIP and dOBIP[a]

	transient absorption			time-resolved fluorescence
time component	OBIP	dOBIP	τ_D/τ_H	OBIP
time1 (ps)		0.18 ± 0.04		
time2 (ps)	0.54 ± 0.05	1.1 ± 0.1	2.0 ± 0.4	
time3 (ps)	3.7 ± 0.4	6.8 ± 0.6	1.8 ± 0.4	<10
time4 (ps)	29 ± 5	47 ± 13	1.6 ± 0.7	21 ± 1
time5 (ps)	133 ± 19	184 ± 33	1.4 ± 0.5	112 ± 1
time6 (ns)	1.2 ± 0.3	3.5 ± 6	2.9 ± 6	0.891 ± 0.016
time7 (ns)				4.4 ± 0.1

[a] The one-to-one correspondence was established on the basis of the spectral similarity of the DADS. The column entitled τ_D/τ_H quantifies the observed kinetic isotope effect as the ratio of the deuterated to ordinary homologous lifetimes. The last column gives the lifetimes coming from the analysis of the time-resolved fluorescence of OBIP, displayed in tentative correspondence with the Trabs data.

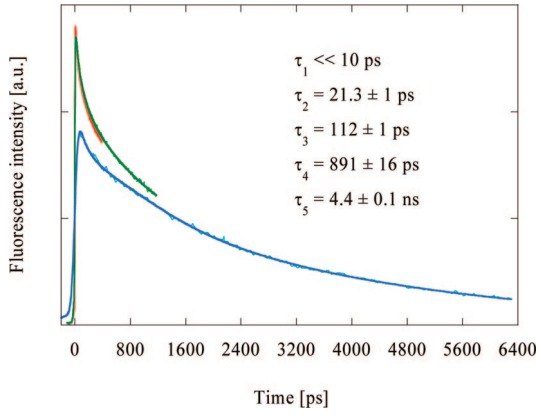

Figure 6. Spectrally integrated fluorescence decays of a solution of OBIP in PBC, after 600 fs excitation at 566 nm, detected by a streak camera. The three kinetic traces correspond to three sweeping rates. The decays were globally fitted to the sum of five exponentials. The best fit includes a short unresolved component (<10 ps) and the following four lifetimes: 21.3 ± 1 ps, 112 ± 1 ps, 891 ± 16 ps, 4.4 ± 0.1 ns.

heterogeneity of the sample (Section 4.2), excited-state deprotonation (Section 4.3), and primary photoprocesses (Section 4.4). The relevance of our findings to the photophobic response of *Blepharisma japonicum* is discussed last (Section 4.5).

4.1. Excited-State Behavior of Free OxyBP and dpOxyBP. It is apparent from Figure 2B that most of the excited-state behavior of OxyBP in PBCE is accounted for by the nanosecond decay and by the plateau. The 1.4 ns component is compatible with reported values for the OxyBP excited-state lifetime in DMSO (1.3,[16] 1 ns[13]) or in ethanol (1.6,[16] 1.8 ns[13]). The difference spectrum of the long-lived species strongly reminds that of the triplet state of OxyBP with its characteristic positive signal around 635 nm.[14,15,35] A slight negative dip nevertheless remains around 650 nm. It is probably due to insufficient discrimination between the 1.4 ns decay, bearing stimulated-emission at 650 nm, and the plateau. Our observation window was indeed limited to a maximum pump−probe delay of 1.4 ns. We therefore conclude that the long-lived species formed in 1.4 ns is the triplet state of OxyBP.

The three short lifetimes of OxyBP in PBCE are quite minor components, which we interpret as a combination of effects. The 0.27 and 3.5 ps components are related to the above-mentioned very slight red shift of the two negative bands (Figure 2A). This phenomenon, which probably arises from a dynamic Stokes shift of the stimulated-emission bands, is interpreted as the relaxation of the solvation cage, which is the case of this sample is some unknown assembly of water, phosphates, sodium cholate, and ethanol molecules, upon excitation of the solute. For comparison, solvation dynamics in water involves three fast components below 900 fs[37] and the average solvation time of ethanol is 16 ps.[38] The very small amplitude of the solvation dynamics is consistent with the weak solvatochromic behavior of OxyBP.[14] The third lifetime, 31 ps, might be compared to a similar weak component observed in the case of free OxyBP in DMSO (15 ps[15]) and previously assigned to a slight change of the nonplanar chiral conformational of the molecule in the excited state.[12,39]

As far as dpOxyBP in WCE is concerned, the main excited-state decay occurs in 4.2 ns. This value is not precisely determined due to our observation window being limited to 1.4 ns. It is in fact possible, as some of our fits suggest, that a long-lived species would be produced in a slightly shorter time range of ca. 3−4 ns. As for OxyBP, the shorter time components (0.22, 3.5 and 55 ps) have rather small amplitudes (Figure 3B) and are associated to what appears as a red shift of the stimulated-emission signal (Figure 3A). We therefore tentatively assign them to solvation dynamics in the heterogeneous WCE medium. It may be noted that peri-deprotonation of OxyBP was achieved with 2.1 mol L^{-1} NaOH. The presence of such a large ion concentration might add longer time components to the overall solvation response.[40] It cannot also be excluded that the 55 ps component is related to a structural relaxation of dpOxyBP, such as the one that was postulated for Hyp (60 ps in ethanol, 80 ps in DMSO).[11]

4.2. Ground-State Heterogeneity of OBIP. We have seen in Section 3.1 that the strong blue shift and narrowing of the fluorescence excitation spectrum of OBIP as compared to its absorption spectrum is not observed in the case of the free chromophore in solution, despite of the spectral similarity of the two systems. Let us also recall that the fluorescence quantum yield of OBIP is smaller than that of OxyBP by a factor of 4. It is therefore quite unlikely that the binding of OxyBP to its natural protein partner opens up new intrinsic deactivation channels, yielding weaker fluorescence emission upon excitation on the low energy edge of the absorption spectrum. It is much more likely that the OBIP sample is actually heterogeneous and that the red part of the absorption spectrum corresponds to a population of chromoprotein undergoing a more efficient quenching of the fluorescent state.

This interpretation is in good agreement with the transient-absorption measurements on OBIP. It is indeed found that the spectrum observed at long times strongly reminds the one of free OxyBP in solution, with a net gain band around 655 nm and a small, flat bleaching contribution in the region of 440 nm. The corresponding lifetimes (1.2 ns for OBIP and 1.4 ns for OxyBP in PBCE) are also similar. Comparable findings were previously reported[13−15] and interpreted in terms of the hetero-

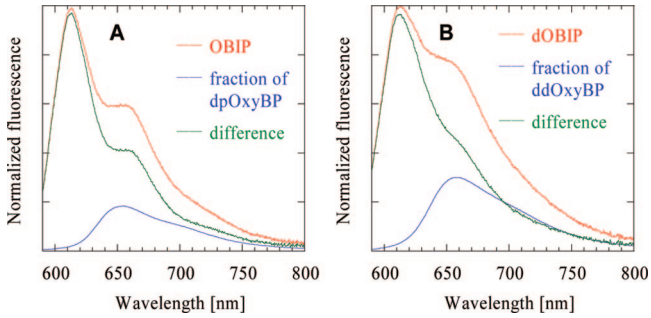

Figure 7. (A) Tentative decomposition of the steady-state fluorescence emission spectrum of OBIP in PBC (red) into the sum of a fraction of peri-deprotonated OxyBP emission (dpOxyBP in WCE, blue) and an OxyBP-like emission (difference spectrum in green). (B) Same procedure applied to dOBIP in dPBC (red) using the fluorescence spectrum of ddOxyBP in dWC (blue).

geneous composition of the OBIP sample. Two populations were then postulated: a reactive one (rOBIP), undergoing a fast photocycle and a nonreactive population (nrOBIP) mostly behaving like the free chromophore in solution. Photodissociation (excited-state decomplexation) was ruled out by energy arguments based on the small steady-state Stokes shift of the OBIP system.[14] The fractions of rOBIP and nrOBIP were previously estimated to 60 and 40%, respectively.[15] Our present results support this view and we assign to rOBIP the first four, subns time components of the global analysis (DADS1 to DADS4) and to nrOBIP the 1.2 ns decay and the plateau (DADS5 and DADS6). The estimation of the fractions of rOBIP and nrOBIP was not repeated here because our method relied upon the measurement of the pure bleaching signal around 560 nm, which is obscured by pump scattering in the present experiments. As we previously suggested,[14] this heterogeneity could in particular arise from different configurations of the chromophore within the protein, such as different binding sites, different interactions between the protein and the five isospectral forms of OxyBP[41] or different orientations of OxyBP inside the protein pocket. Different protein conformations or natures could also be involved but no experimental proof of any of those hypotheses is available to us at the moment.

4.3. Excited-State Deprotonation of OBIP. It is quite intriguing that the fluorescence emission spectrum of OBIP displays a less pronounced vibrational structure than the corresponding fluorescence excitation spectrum, with a shallower minimum between the two emission maxima and smaller intensity ratio of the first to second maxima. This dissymmetry is much more obvious for dOBIP. One can note that the fluorescence emission spectrum of dpOxyBP in WCE displays a broad maximum in the same spectral region as the secondary maximum of OBIP's fluorescence (around 650 nm). We thus may tentatively propose that the fluorescence emission spectrum of OBIP is in fact the superposition of two contributions: a conveniently red-shifted and broadened OxyBP-like emission and an associated peri-deprotonated OxyBP emission. The same hypothesis would also hold for dOBIP with an even larger contribution of the emission of the dedeuterated species. In order to show in a qualitative way that such a decomposition could be possible, we subtracted from the (normalized) emission spectrum of OBIP in PBC a fraction of the (normalized) emission spectrum of dpOxyBP in WCE. The fraction of dpOxyBP emission was loosely adjusted in such a way that the difference spectrum may appear as an improved mirror image of the fluorescence excitation spectrum (see Figure 7A). The same procedure was performed on dOBIP's fluorescence with the help of the emission spectrum of ddOxyBP in dWC (Figure 7B). We stress on the fact that Figure 7 is not presented as a proof but rather as a visual guide supporting our hypothesis. It is also true that the real fluorescence spectrum of OBIP putatively bearing a peri-deprotonated chromophore would likely be somewhat different from the emission spectrum of dpOxyBP in WCE used here. Since the fluorescence excitation spectra of OBIP and dOBIP do not reveal the presence of peri-deprotonated species in the ground state, the interesting consequence of our proposal is that the occurrence of the peri-deprotonated emission would arise in both OBIP and dOBIP cases from an excited-state deprotonation process.

It was indeed shown in Section 3.1 that the absorption and fluorescence spectra of dpOxyBP are red-shifted as compared to those of OxyBP, the same being true for ddOxyBP as compared to dOxyBP. Such a red shift is assignable to a lowering of the perihydroxyl pK_a in the excited state. Application of the Förster cycle[27] yields $\Delta pK_a = pK_a^* - pK_a = -2.3$ for OxyBP and -2.2 dOxyBP, the 0−0 transition location being estimated by the average wavenumber position of the absorption and fluorescence maxima. Such values are similar to the ΔpK_a value of -2.7 reported for the perihydroxyl groups of Hyp by Eloy et al.[24] It may be argued that since the pK_a of the OxyBP perihydroxyl groups is situated around 11 in solution (reported value for Hyp[24,25] and blepharismin[42]), one would expect the corresponding excited-state pK_a in the range of 8−9. In order to explain that some excited-state deprotonation of OBIP occurs at pH 7.4, one would therefore need to hypothesize that the effective perihydroxyl pK_a of OxyBP is somewhat reduced to a lower value upon binding to the protein, as is for example the case for the phenol group of the chromophore covalently bound to the Photoactive Yellow Protein.[43] On the other hand, in the absence of photoinduced deprotonation of OxyBP in solution, the increase of its fluorescence yield upon deuteration (Figure 1B and Table 1) remains to be understood. One might think that this isotope effect has the same origin as that observed for the deprotonated form dpOxyBP. Table 1 indeed shows that the fluorescence yield of ddOxyBP is almost twice larger than that of dpOxyBP. Similar findings were in particular reported for xanthene dyes.[44] Deuteration of the solvent hydroxyl groups (water, alcohols) was found to reduce the internal conversion rate constant of the deprotonated dye by about 1.6, revealing the role of the solute−solvent hydrogen-bonding interaction in the non radiative relaxation. The present observation might thus indicate that hydrogen-bonding plays a role in the nonradiative relaxation of OxyBP in solution.

An additional experimental element in favor of excited-state deprotonation of OBIP is the occurrence of a substantial (39.6%) 4.4 ns time component in the integrated fluorescence decay reported in Section 3.4. Such a long lifetime does not match the excited-state decay time of OxyBP in PBCE provided by the present transient absorption experiment (1.4 ns) nor the previously reported fluorescence lifetimes of OxyBP in organic solvents (between 1 and 1.8 ns).[13,16] It is on the other hand much more comparable to the excited-state decay time of peri-deprotonated OxyBP in WCE measured by our transient absorption setup, that is, 4.2 ns. Since the transient-absorption spectra of OBIP do not explicitly reveal the spectral features of deprotonated OxyBP within the 1.4 ns time window of the experiment, it may be supposed that excited-state deprotonation of OBIP would likely occur in the nanosecond time scale. The transient-absorption experiment evidenced a component of 1.2 ns while time-resolved fluorescence pointed to ∼0.9 ns. The

lifetime of the putative excited-state deprotonation of OBIP would then lie in the vicinity of those times.

4.4. Primary Photoresponse of rOBIP. As presented in Section 4.2, the first level of interpretation of our transient-absorption results consists in assigning to the reactive population (rOBIP) the first four time components of the global analysis, while the remaining two are attributed to the nonreactive population (nrOBIP). DADS4, which is the longest-lived (133 ps) species associated to rOBIP, displays a clear peak at 676 nm (Figure 4B) that we assign to a characteristic contribution of the OxyBP radical cation ($OxyBP^{\bullet+}$), as was previously shown by direct comparison with an $OxyBP^{\bullet+}$ difference spectrum obtained by photooxidation of OxyBP by p-benzoquinone (BZQ)[15] (let us note that this spectrum also contains a contribution from the BZQ radical anion, $BZQ^{\bullet-}$). A good superposition is also obtained for the present results if the radical cation spectrum is shifted by 8 nm toward the red in order to compensate for a solvatochromic shift between the two systems (not shown). The photooxidation experiment was indeed done in ethanol where the absorption of OxyBP is blue-shifted as compared to the chromoprotein.

What the present transient-absorption and time-resolved fluorescence (see Section 3.4) results suggest is that DADS4 not only bears the spectral signature of the oxyblepharismin radical cation but also that of an emitting species. Although electron transfer is believed to be involved in the excited-state dynamics of rOBIP, it cannot be concluded that an irreversible electron transfer from OxyBP to a nearby electron acceptor (the disulphide bridge of a cystine was previously proposed by Angelini et al.[16]) takes place and simply yields a ground-state photoproduct. In order to account for the observation of an emitting species that coexists with the radical cation signature and simultaneously decays with it, we propose that an equilibrium is actually reached between an electronically excited, emitting, precursor state and a charge-transfer state.

Such a situation was described some years ago by the group of Mataga in the context of fluorescence quenching within hydrogen bond (HB) complexes between pairs of conjugated π-electron systems in nonpolar solvents.[45,46] One of the molecules acts as the electron donor, its ionization potential being substantially lowered by the hydrogen bonding,[47] while the other one is the electron acceptor. Mataga proposed that upon excitation the fluorescence of the donor can be efficiently quenched by the formation of a kind of nonfluorescent exciplex. A first curve crossing in the locally excited (LE) state leads to a charge-transfer (CT) state, which itself crosses the ground-state potential energy curve and induces back charge recombination down to the ground state.[45] Martin et al. showed that an equilibrium could actually be reached between the LE state and the CT state. The equilibrium is established in less than 10 ps in the case of the 7*H*-dibenzocarbazole-pyridine complex.[48] On the basis of ab initio calculations by Tanaka and Nishimoto,[49] Miyasaka et al. published a model in which the coordinate along which the electron transfer proceeds is the shift of the hydrogen bond proton toward the acceptor.[50] Two limiting cases were proposed. If the shift is large (1-pyrenol−pyridine case), crossing with the ground-state potential occurs close to the minimum of the CT state and charge recombination is fast. If the proton shift is small (1-aminopyrene−pyridine case), crossing with the ground-state potential occurs at a higher energy, the lifetime of the CT species is longer and the equilibrium with the LE state can be observed. It is interesting to note that recent advanced calculations on the indole−pyridine HB complex by Sobolewski and Domcke[51] confirm the role of a charge-transfer state connecting both the LE and ground states through conical intersections and of the proton shift as the reaction coordinate along which excited-state deactivation proceeds. These authors in fact advocate the relevance of such HB photochemistry to explain not only the photostability of DNA base pairs[52] but also that of polypeptides.[53]

SCHEME 2: Kinetic Model Proposed to Explain the Excited-State Behavior of rOBIP[a]

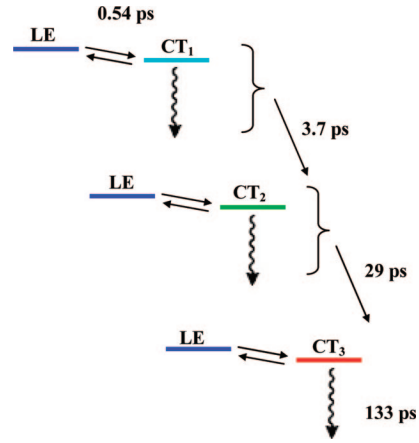

[a] An equilibrium is supposed to be reached between the locally-excited state (LE) and a charge-transfer state (CT). The CT state nonradiatively decays to the initial ground state (undulated arrow) through charge recombination. As the protein relaxes the spectrum of the CT state slightly evolves (from CT_1 to CT_3) and its decay rate slows down.

We here tentatively propose that this framework could apply to the OBIP chromoprotein, the hydrogen-bond complex and the nonpolar environment being provided by the protein. The equilibrium between the LE and CT states would explain the coexistence within DADS4 of the stimulated-emission contribution and the radical cation signature, respectively. In order to explain the occurrence of three kinetic steps preceding the decay of DADS4, we additionally propose that the equilibrium is reached in the subps regime (0.54 ps component) or nonlinearly with both the 0.54 and 3.7 ps components. The following lifetimes (3.7 and 29 ps, or 29 ps alone) could be assigned to the relaxation of the protein pocket induced by the change of electronic distribution within the donor−acceptor pair. The probed dynamics could indeed be viewed as a LE ⇔ CT charge-transfer reaction occurring on an excited surface defined by the proton-shift coordinate on the one hand and the protein pocket restructuring coordinate on the other hand, similarly to the description of intramolecular CT reactions in solution involving both intramolecular and solvent coordinates.[54] For OBIP, one would thus hypothesize that along the protein relaxation coordinate the CT potential well would evolve, preventing the CT state from fast return to the ground state. This relaxation would make the spectral signature of the radical cation sharper and reduce the charge recombination rate. It is interesting to note that the dynamics measured in the case of deuterated OBIP were slowed down by a factor of 1.6 to 2 as far as rOBIP is concerned (see Section 3.3 and Table 2, time1 to time4). This kinetic isotope effect may be considered as an element in favor of the Mataga−Miyasaka model presented above, in which electron transfer is coupled to the shift of the hydrogen-bond proton.

The feasibility of this idea was tested at an approximate, semiquantitative level with the simplified kinetic model depicted in Scheme 2. The initial excited state (LE, blue line) reaches

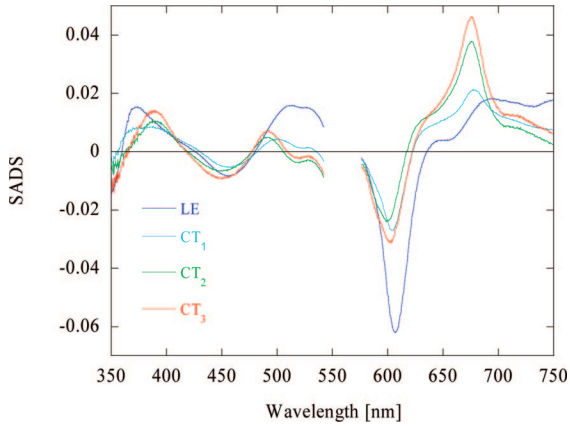

Figure 8. Species-associated difference spectra (SADS) corresponding to the analysis of the transient-absorption spectra of rOBIP (reactive population, see Section 4.2) in terms of the kinetic model depicted in Scheme 2.

an equilibrium with the charge-separated species (CT_1, cyan line) in 0.54 ps. As CT_1 decays to the ground state by charge recombination while the hypothesized response of the protein environment proceeds, both its spectrum and recombination rate evolve. In 3.7 ps CT_1 becomes CT_2 (green line) which turns into CT_3 (red line) in 29 ps. CT_3 finally decays to the initial ground-state in 133 ps. This model could be used to transform the DADS into species-associated difference spectra (SADS) according to a method described by Ernsting et al.[33] The parameters defining the model were semimanually adjusted so as to approximately satisfy the following constraints: (i) the SADS of the three CT species should not exhibit stimulated emission and (ii) the bleaching contribution of each SADS should be identical. We wish to stress the fact that this procedure was not an actual target analysis because the parameters were not fully optimized and because the constraints were evaluated by visual inspection of the SADS only. Our goal was limited to showing that the type of model described by Scheme 2 could provide an acceptable description of the data. Figure 8 displays a set of SADS roughly satisfying the above-mentioned constraints. The amplitude of the main negative peak of SADS1 (LE) is larger than that of the other three because it is the only one bearing a stimulated-emission contribution on its red side. The characteristic $OxyBP^{\bullet+}$ peak around 675 nm of the CT species is seen to narrow, slightly shift toward the blue and gain intensity, from SADS2 to SADS4, as protein relaxation proceeds.

The 675 nm structure of SADS4 can readily be subtracted out with the help of the, properly shifted, $OxyBP^{\bullet+}-BZQ^{\bullet-}$ spectrum[15] mentioned above (data not shown). Although the obtained difference spectrum shows the expected negative contribution of the p-benzoquinone radical anion around 450 nm,[55] it does not allow the identification of a possible electron acceptor within OBIP. The conjugated, hydrogen-bond acceptor, electron acceptor of OBIP, required within the Mataga−Misayaka model, might hypothetically be a histidine residue. It has indeed been reported that this molecule may act as an electron acceptor in proteins and yield an absorption band around 360 nm,[56] which in our results would possibly be masked by a bleaching feature in the same region.

It is interesting to note that the initial spectrum of rOBIP (SADS1) is substantially different from that of nrOBIP (see Figure 4A for a time delay of 500 ps, or the sum of DADS5 and DADS6 in Figure 4B), which reminds free OxyBP in solution (Figure 2). The rather flat transient-absorption band of rOBIP-SADS1, extending from 688 to 750 nm, together with the absence of net gain band around 655 nm could in fact be observed in the case of an artificial complex of OxyBP with alpha-Crystallin, the major protein in charge of maintaining transparency and proper refractive index of the eye lens.[23] It may be hypothesized that the special shape of rOBIP-SADS1 reveals a particular interaction of OxyBP with its protein environment, also found in the complex with alpha-Crystallin but absent in the complex with human serum albumin.[14] This sole interaction is however not sufficient to induce the characteristic fast evolution of OBIP because this one was not observed in the case of the alpha-Crystallin complex.[23] This difference confirms the previously commented specific nature of the OBIP photoinduced behavior.[14]

4.5. Photophobic Response of *Blepharisma japonicum*. As noted in a previous report,[15] the dynamics associated with rOBIP is likely too fast to generate any biologically useful signaling state, and hence may not be responsible for the photophobic response of *B. japonicum*. We proposed that the fast photocycle of rOBIP could in fact be a fast efficient deactivation pathway of the excited state, providing a sunscreen mechanism that protects *B. japonicum* from continuous irradiation. Let us indeed remind that the active pigment of the dark-adapted form of the cell, blepharismin (BP, Scheme 1), is highly phototoxic[57] and that the OBIP chromoprotein, bearing OxyBP as a chromophore, only exists in the light-adapted form of the organism.[4] This hypothesis may be maintained although one should keep in mind that the present experiments were done in vitro, in the absence of possible protein partners. It could also be argued that a less costly sunscreen would be constituted by stacked OxyBP molecules, that would deactivate very fast, since it is known that the pigment is contained in large concentration in specialized granules.[58,59] On the other hand, we previously suggested that continuous visible excitation induces artificial complexes of OxyBP with alpha-Crystallin to pack, leading to fluorescence quenching of OxyBP.[23] If such a process were active for OBIP in vivo, a particular type of sunscreen could even build up in blue *B. japonicum*, as a result of irradiation. The fast photocycle of rOBIP would however constitute a more immediate solar protection of blue *B. japonicum*, independent of the stacking condition of the pigment. It would in any case be considered as potential complementary sunscreen, in addition to any other protection mechanism. Let us finally mention that no comparative data is presently available for the red blepharismin binding protein, which was once isolated from red *B. japonicum* cells[58,60] but apparently releases its chromophore much more easily than OBIP (G. Checcucci, unpublished results).

If the fast photocycle of rOBIP were indeed not to be linked with the photophobic response of *B. japonicum*, the real primary photoprocess at the origin of the photophobic response of *B. japonicum* would have to be looked for in another direction. It has to be recalled that action spectroscopy demonstrated that the OxyBP molecules trigger the photophobic response of *B. japonicum*.[4,5] It was also claimed that irradiation of the cell induces an intracellular pH jump.[61−63] It could therefore be suggested that nrOBIP chromoproteins would just release protons upon excitation and thereby trigger the transduction chain, as reported for the photoreceptor of another ciliate, *Stentor coeruleus*.[64,65] This hypothesis is compatible with our present results since, as discussed in Section 4.3, we indirectly infer that OBIP undergoes excited-state peri-deprotonation. Deprotonation would likely take place during the excited-state lifetime of nrOBIP, that is, in the nanosecond/subnanosecond regime. Alternatively, one could consider that unbound OxyBP mol-

ecules may be the source of photorelease protons, possibly from their triplet state as was suggested by J. Petrich in the case of hypericin.[66]

5. Conclusion

The present femtosecond transient-absorption and picosecond fluorescence experiments performed on OBIP bring new insights into the photoinduced dynamics of this chromoprotein, as compared to formerly reported works.[11,13−15] The fast formation of a characteristic 675 nm absorption band, assigned to the OxyBP radical cation, has here been resolved and seen to occur in the subpicosecond regime with a lifetime of 0.54 ps. The band then decays while sharpening with time constants of 3.7 and 29 ps, and finally disappears with a lifetime of 133 ps. We additionally demonstrated that a stimulated-emission signal, also detected by time-resolved fluorescence, coexists with this band at all times of its evolution.

Our interpretation of the data confirms in the first place the previously proposed model involving two independent classes of chromoproteins: while the reactive population rOBIP undergoes the fast dynamics, the nonreactive species nrOBIP mostly behaves like the free chromophore in solution with a nanosecond decay and a net gain band around 655 nm. The difference absorption spectrum of the initial excited-state of rOBIP could be resolved for the first time by the present experiments and has been shown to be different from the one of nrOBIP. Its particular structure with a flat transient-absorption band in the red part of the spectrum and no net gain band around 655 nm is assigned to a specific type of interaction of the chromophore with its protein environment. The photophysics of rOBIP has been refined in terms of a reversible excited-state intermolecular electron transfer (equilibrium between LE and CT states) followed by electron recombination in the ground state. The spectrum of the CT species is supposed to sharpen as a result of protein relaxation while the recombination rate decreases. Within the framework of the theory developed by Mataga and Miyasaka to explain the fluorescence quenching of aromatic hydrogen-bonded donor−acceptor pairs in nonpolar solvents,[50] we hypothesize that OxyBP is involved in a hydrogen-bond interaction with an as yet unknown electron acceptor and that the shift of the proton involved in the hydrogen bond is the reaction coordinate.

As previously discussed,[15] we propose that the fast dynamics of rOBIP may act, through an efficient deactivation of the excited state, as a sunscreen mechanism aimed at protecting *B. japonicum* against excessive irradiation. On the basis of a comparative study including steady-state and time-resolved fluorescence of OBIP as well as transient absorption spectroscopy of peri-deprotonated free OxyBP in solution, we further hypothesize that the triggering process of the photophobic response of the organism could be an excited-state deprotonation of the so-called nrOBIP class of chromoprotein, occurring in the nanosecond regime.

Acknowledgment. The authors acknowledge financial support from the ANR (French National Agency for Research) to the "Femtomotile" project (ANR-05-BLAN-0188-01).

References and Notes

(1) van der Horst, M. A.; Hellingwerf, K. J. *Acc. Chem. Res.* **2004**, *37*, 13.
(2) Losi, A. *Photochem. Photobiol.* **2007**, *83*, 1283.
(3) Ghetti, F. *Biophysics of Photoreceptors and Photomovements in Microorganisms*; Plenum Press: New York, 1991; p 257.
(4) Matsuoka, T.; Matsuoka, S.; Yamaoka, Y.; Kuriu, T.; Watanabe, Y.; Takayanagi, M.; Kato, Y.; Taneda, K. *J. Protozool.* **1992**, *39*, 498.
(5) Checcucci, G.; Damato, G.; Ghetti, F.; Lenci, F. *Photochem. Photobiol.* **1993**, *57*, 686.
(6) Matsuoka, T.; Sato, M.; Maeda, M.; Naoki, H.; Tanaka, T.; Kotsuki, H. *Photochem. Photobiol.* **1997**, *65*, 915.
(7) Matsuoka, T.; Tokumori, D.; Kotsuki, H.; Ishida, M.; Matsushita, M.; Kimura, S.; Itoh, T.; Checcucci, G. *Photochem. Photobiol.* **2000**, *72*, 709.
(8) Giese, A. C. *Blepharisma: The Biology of a Light-Sensitive Protozoan*; Stanford University Press: Stanford, CA, 1973.
(9) Giese, A. C. *J. Cell. Comp. Physiol.* **1946**, *28*, 119.
(10) Spitzner, D.; Höfle, G.; Klein, I.; Pohlan, S.; Ammermann, D.; Jaenicke, L. *Tetrahedron Lett.* **1998**, *39*, 4003.
(11) Plaza, P.; Mahet, M.; Tchaikovskaya, O. N.; Martin, M. M. *Chem. Phys. Lett.* **2005**, *408*, 96.
(12) Falk, H. *Angew. Chem.* **1999**, *38*, 3116.
(13) Plaza, P.; Mahet, M.; Martin, M. M.; Angelini, N.; Malatesta, M.; Checcucci, G.; Lenci, F. *Photochem. Photobiol. Sci.* **2005**, *4*, 754.
(14) Mahet, M.; Plaza, P.; Martin, M. M.; Checcucci, G.; Lenci, F. *J. Photochem. Photobiol. A* **2007**, *185*, 345.
(15) Plaza, P.; Mahet, M.; Martin, M. M.; Checcucci, G.; Lenci, F. *J. Phys. Chem. B* **2007**, *111*, 690.
(16) Angelini, N.; Quaranta, A.; Checcucci, G.; Song, P.-S.; Lenci, F. *Photochem. Photobiol.* **1998**, *68*, 864.
(17) Checcucci, G.; Takada, Y.; Matsuoka, T. *Mem. Fac. Sci. Kochi Univ. D* **2001**, *22*, 39.
(18) Chattoraj, M.; King, B. A.; Bublitz, G. U.; Boxer, S. G. *Proc. Natl. Acad. Sci. U.S.A.* **1996**, *93*, 8362.
(19) Coetzee, J. F.; Ritchie, C. D. *Solute–Solvent Interactions*; M. Dekker: New York, 1969; p 663.
(20) Krezel, A.; Bal, W. *J. Inorg. Chem.* **2004**, *98*, 161.
(21) Glasoe, P. K.; Long, F. A. *J. Phys. Chem.* **1960**, *64*, 188.
(22) Checcucci, G.; Shoemaker, R. S.; Bini, E.; Cerny, R.; Tao, N.; Hyon, J.-S.; Gioffré, D.; Ghetti, F.; Lenci, F.; Song, P.-S. *J. Am. Chem. Soc.* **1997**, *119*, 5762.
(23) Youssef, T.; Brazard, J.; Ley, C.; Lacombat, F.; Plaza, P.; Martin, M. M.; Sgarbossa, A.; Checcucci, G.; Lenci, F. *Photochem. Photobiol. Sci.* **2008**, *7*, 844.
(24) Eloy, D.; Le Pellec, A.; Jardon, P. *J. Chim. Phys.* **1996**, *93*, 442.
(25) Leonhartsberger, J. G.; Falk, H. *Monat. Chem.* **2002**, *133*, 167.
(26) Vollhardt, P.-C.; Schore, N.-E. *Organic Chemistry*, 4th ed.; W.H. Freeman: New York, 2003.
(27) Valeur, B. *Molecular Fluorescence. Principles and Applications*; Wiley-VCH: Weinheim, 2002.
(28) Karstens, T.; Kobs, K. *J. Phys. Chem.* **1980**, *84*, 1871.
(29) Frank, A. J.; Otvos, J. W.; Calvin, M. *J. Phys. Chem.* **1979**, *83*, 716.
(30) Magde, D.; Brannon, J. H.; Cremers, T. L.; Olmsted, J. *J. Phys. Chem.* **1979**, *83*, 696.
(31) Ley, C.; Brazard, J.; Lacombat, F.; Plaza, P.; Martin, M. M.; Kraus, G. A.; Petrich, J. W. *Chem. Phys. Lett.* **2008**, *457*, 82.
(32) Henry, E. R.; Hofrichter, J. *Methods Enzymol.* **1992**, *210*, 129.
(33) Ernsting, N. P.; Kovalenko, S. A.; Senyushkina, T.; Saam, J.; Farztdinov, V. *J. Phys. Chem. A* **2001**, *105*, 3445.
(34) Dai Hung, N.; Plaza, P.; Martin, M. M.; Meyer, Y. H. *Appl. Opt.* **1992**, *31*, 7046.
(35) Ghetti, F.; Checcucci, G.; Lenci, F.; Heelis, P. F. *J. Photochem. Photobiol. B* **1992**, *13*, 315.
(36) Kraus, G. A.; Zhang, W.; Fehr, M. J.; Petrich, J. W.; Wannemuehler, Y.; Carpenter, S. *Chem. Rev.* **1996**, *96*, 523.
(37) Jimenez, R.; Fleming, G. R.; Kumar, P. V.; Maroncelli, M. *Nature* **1994**, *369*, 471.
(38) Horng, M. L.; Gardecki, J. A.; Papazyan, A.; Maroncelli, M. *J. Phys. Chem.* **1995**, *99*, 17311.
(39) Pieroni, O.; Plaza, P.; Mahet, M.; Angelini, N.; Checcucci, G.; Malatesta, M.; Martin, M. M.; Lenci, F. *Photochem. Photobiol.* **2005**, *81*, 1343.
(40) Chapman, C. F.; Maroncelli, M. *J. Phys. Chem.* **1991**, *95*, 9095.
(41) Maeda, M.; Naoki, H.; Matsuoka, T.; Kato, Y.; Kotsuki, H.; Utsumi, K.; Tanaka, T. *Tetrahedron Lett.* **1997**, *38*, 7411.
(42) Losi, A.; Vecli, A.; Viappiani, C. *Photochem. Photobiol.* **1999**, *69*, 435.
(43) Demchuk, E.; Genick, U. K.; Woo, T. T.; Getzoff, E. D.; Bashford, D. *Biochemistry* **2000**, *39*, 1100.
(44) Martin, M. M.; Lindqvist, L. *Chem. Phys. Lett.* **1973**, *22*, 309.
(45) Mataga, N. *Pure Appl. Chem.* **1984**, *56*, 1255.
(46) Mataga, N.; Miyasaka, H. *Electron Transfer-From Isolated Molecules to Biomolecules, Part 2*; Wiley-Interscience: New York, 1999; p 431.
(47) Martin, M. M.; Grand, D.; Ikeda, N.; Okada, T.; Mataga, N. *J. Phys. Chem.* **1984**, *88*, 167.

(48) Martin, M. M.; Ikeda, N.; Okada, T.; Mataga, N. *J. Phys. Chem.* **1982**, *86*, 4148.
(49) Tanaka, H.; Nishimoto, K. *J. Phys. Chem.* **1984**, *88*, 1052.
(50) Miyasaka, H.; Tabata, A.; Ojima, S.; Ikeda, N.; Mataga, N. *J. Phys. Chem.* **1993**, *97*, 8222.
(51) Sobolewski, A. L.; Domcke, W. G. *J. Phys. Chem. A* **2007**, *111*, 11725.
(52) Sobolewski, A. L.; Domcke, W.; Hattig, C. *Proc. Natl. Acad. Sci. U.S.A.* **2005**, *102*, 17903.
(53) Sobolewski, A. L.; Domcke, W. *ChemPhysChem* **2006**, *7*, 561.
(54) Kim, H. J.; Hynes, J. T. *J. Photochem. Photobiol. A* **1997**, *105*, 337.
(55) Shida, T. *Electronic Absorption Spectra of Radical Ions*; Elsevier: Amsterdam, 1988.
(56) Faraggi, M.; Klapper, M. H.; Dorfman, L. *J. Phys. Chem.* **1978**, *82*, 508.
(57) Terazima, M. N.; Iio, H.; Harumoto, T. *Photochem. Photobiol.* **1999**, *69*, 47.
(58) Matsuoka, T.; Tsuda, T.; Ishida, M.; Kato, Y.; Takayanagi, M.; Fujino, T.; Mizuta, S. *Photochem. Photobiol.* **1994**, *60*, 598.
(59) Sgarbossa, A.; Checcucci, G.; Lenci, F. *Photochem. Photobiol. Sci.* **2002**, *1*, 459.
(60) Matsuoka, T.; Murakami, Y.; Kato, Y. *Photochem. Photobiol.* **1993**, *57*, 1042.
(61) Matsuoka, T.; Muraka, Y.; Furukohri, T.; Ishida, M.; Taneda, K. *Photochem. Photobiol.* **1992**, *56*, 399.
(62) Fabczak, H.; Fabczak, S.; Song, P.-S.; Checcucci, G.; Ghetti, F.; Lenci, F. *J. Photochem. Photobiol. B* **1993**, *21*, 47.
(63) Matsuoka, T.; Kotsuki, H. *J. Exper. Zool.* **2001**, *289*, 467.
(64) Song, P.-S.; Walker, E. B.; Auerbach, R. A.; Wilse, G. *Biophys. J.* **1981**, *35*, 551.
(65) Walker, E. B.; Yoon, M.; Song, P.-S. *Biochim. Biophys. Acta* **1981**, *634*, 289.
(66) Fehr, M. J.; McCloskey, M. A.; Petrich, J. W. *J. Am. Chem. Soc.* **1995**, *117*, 1833.

JP805815E